Desalination and Water Treatment
www.deswater.com
6 (2009) 252–268

Adsorption, kinetic and equilibrium studies on removal of basic dye from aqueous solutions using hydrolyzed Oak sawdust

M.M. Abd El- Latif*, Amal M. Ibrahim

Mubarak City for Scientific Research and Technology Applications, Institute of Advanced Technologies and New Materials, Fabrication Technology Department, Alexandria, Egypt
Tel./Fax +20 34593414; email: amona1911@yahoo.com

Received 22 June 2008; accepted 2 April 2009

ABSTRACT

Oak sawdust (SD), which is the main waste from furniture industry in Egypt, has been used as an adsorbent without treatment or it was treated with 0.1 N sodium hydroxide (SD1) and 0.1 N sulphuric acid (SD2). Different adsorbents were characterized by SEM, TGA and FTIR to clarify the effect of treatment on the adsorption process. Oak sawdust and different treated Oak sawdust have been used for the removal of methylene blue dye from aqueous solutions. Batch adsorption experiments were performed as a function of pH, adsorbent dose, agitation speed, contact time and initial dye concentration. The optimum pH required for maximum adsorption was found to be 8. The experimental equilibrium adsorption data are tested for Langmuir, Freundlich and Temkin isotherms. Results indicate the following order to fit the isotherms: Langmuir > Temkin >>> Freundlich adsorption. Kinetics data were modeled using the pseudo-first and pseudo-second order, Elovich equations and intra-particle diffusion models. The results indicate that the second-order model best describes adsorption kinetic data with regard to the intra-particle diffusion rate. Thermodynamic parameters ΔH, ΔS and ΔG have been calculated for each type of adsorbents. Positive value of ΔH and negative value of ΔG show endothermic and spontaneous nature of adsorption respectively, also activation energy Ea has been calculated.

Keywords: Adsorption; Isotherms; Kinetics; Cationic dye; Sawdust

1. Introduction

The environmental impact of the dyes present in the wastewater streams of many industrial sectors, such as dyeing, textile, tannery and the paint industry, has drawn a lot of attention, emphasizing the necessity for their removal. As a result of the low biodegradability of dyes, the conventional biological treatment process is not very effective in treating dye wastewater [1]. Some of the physicochemical methods that have been employed to remove dyes from wastewater include chemical precipitation, coagulation and oxidation. However, these methods are not economical. Adsorption seems to offer the best prospects over the other treatment techniques but it is expensive [2]. Activated carbon is the most efficient adsorbent used to date, but its high cost limits its applicability. Research is currently focusing on the use of low cost commercially available organic materials as viable substitutes for activated carbon; in fact, sawdust, a relatively abundant and inexpensive material, has been extensively investigated as an adsorbent for removing contaminants from water [3]. Other adsorbent materials that have been studied including wood and agricultural

*Corresponding author

residues, untreated or treated in various ways [4]. Among the untreated materials that have been investigated, wood shavings are commonly used as an adsorbent, especially for basic dyes, with capacity varying according to the structure of the dye and the mesh size [5]. Many agricultural residues, such as wheat straw, wood chips and corncobs, have been used successfully to adsorb individual dyes and dye mixtures in textile effluent [6]. Removal of methylene blue (MB) and other basic dyes has been carried out using coir pith, an unwanted by-product from the coir processing industry [7], banana/orange peels [8] and palm-fruit bunch particles [9,10]. Formaldehyde- and concentrated sulphuric acid-treated sawdust and dilute acid-hydrolyzed charred sawdust have been successfully used as adsorbents for a variety of dyes [1,3]. Cellulose-based anionic dye adsorbents have been prepared from agricultural residues (e.g. wood sawdust) treated with cross-linked polyethylenimine [11]; also, carbonized agricultural wastes such as coir pith [12], cassava peel [13], bagasse [14] and kudzu [15] have been utilized successfully for the removal of dyes from aqueous solutions.

The aim of this work is to investigate the possibility of Oak sawdust, the inexpensive by-product of furniture manufacturing company, to be used as an adsorbent for the removal of basic dyes.

Oak sawdust (SD), 0.1 N sodium hydroxide Oak treated sawdust (SD1) and 0.1 N sulphuric acid-treated Oak sawdust (SD2) were used as adsorbents to remove the MB dye from aqueous solution. The kinetic data and equilibrium data on batch adsorption studies were carried out to understand the adsorption process. The effect of adsorption parameters such as pH, adsorbent dosage, agitation speed, contact time and initial dye concentration by using these low cost adsorbents were also reported. Finally, the thermodynamic data were performed for interpretation of results.

2. Materials and methods

2.1. Materials

Methylene blue (Nice Chemicals Pvt. Ltd., Cochin). Methylene blue, $C_{16}H_{18}N_3SCI \cdot 3H_2O$, is a cationic dye. The structure of this dye is shown in Fig. 1. The stock dye solution was prepared by dissolving 1 g of MB in 1000 mL distilled water to obtain 1000 ppm dye used for preparing different initial dye concentrations. The concentration of MB remaining in the supernatant after and before adsorption was determined with a 1.0 cm light path quartz cells using spectrophotometer (Perkin Elmer model GBC 902) at λ_{max} of 665 nm. For

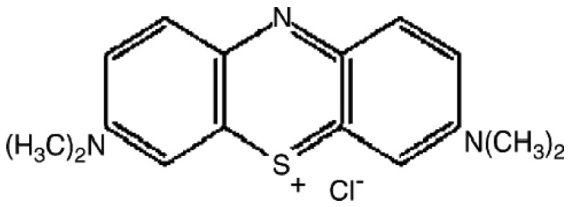

Fig. 1. Structure of methylene blue dye.

hydrolyzed sawdust throughout the experiment, sulphuric acid and sodium hydroxide solutions were used. For pH adjustment throughout the experiment, hydrochloric acid and/or sodium hydroxide solutions were used as necessary.

2.2. Adsorbent preparation and characterization

The Oak sawdust used was obtained from a local furniture manufacturing company, as a suitable source for full-scale/industrial applications. Oak sawdust was used as an adsorbent for the removal of MB. Oak sawdust was washed with distilled water to remove the water-soluble impurities and surface adhered particles, dried in a digital dryer of (Carbolite, Aston Lane, Hope Sheffield, 5302RP, England) for 24 h at 105°C to get rid of the moisture and other volatile impurities and sieved using sieve analyzer (AS200 Retsch, Germany)to different particle size ranges 45–500 μm. The material after sieving in the range 125–250 μm is isolated and divided into three parts: The first part was used as it is for biosorption of MB; it was labeled by (SD). The second part was placed in a conical flask contains 0.1 N NaOH solution at a liquid to solid ratio of 10:1 with 200 rpm agitation speed using orbital shaker (yellow line Os10 Control, Germany) for 2 h at room temperature. The excess alkaline solutions were decanted, and the alkaline hydrolyzed Oak sawdust was washed continuously with distilled water until the pH of the washing water became less than 8 using pH meter (Denver Instrument Co., USA). Finally, the base treated Oak sawdust was dried at 105°C for 6 h (SD1) using digital dryer. The third part was placed in a conical flask contains 0.1 N H_2SO_4 solution at a liquid to solid ratio of 10:1 with 200 rpm agitation speed using orbital shaker for 2 h at room temperature. The excess acidic solutions were decanted, and the acidic hydrolyzed Oak sawdust was washed continuously with distilled water until the pH of the washed water became more than 6. Finally, the acidic treated Oak sawdust was dried at 105°C for 6 h (SD2). The yield from each prepared biosorbent was calculated from the following equation:

$$(W_i - W_f)/W_i \quad (1)$$

where W_i is the mass of material before treated (g), W_f is the mass of material after treatment (g).

The adsorbents were characterized with a number of methods includes SEM, TGA and FTIR.

2.3. Adsorption studies

Batch adsorption experiments were carried out at room temperature (25 ± 2°C). Exactly 100 mL of cationic dye solution of known initial concentration was shaken at the certain agitation speed with a required dose of adsorbents for a specific period of contact time in an orbital shaker, after noting down the initial pH of the solution to the optimum pH. The pH of the solutions were adjusted to the required value by adding either 0.1 M HCl or 0.1 M NaOH solution. After equilibrium, the final concentration (C) was measured. The percentage removal of dye were calculated using the following relationship:

$$\% \text{ Removal} = ((C_o - C)/C_o) \times 100 \quad (2)$$

where C_o and C (both in mg/L) are the initial dye concentration and the dye concentration at any time, respectively.

The adsorption capacity q (mg/g) at any time was calculated by mass balance relationship equation as follows:

$$q = (C_o - C) \times (V/W) \quad (3)$$

where V is the volume of the solution (L), W is the mass of adsorbent (g).

2.3.1. Adsorption parameters

1. Adsorbent dose (0.1, 0.25, 0.5, 1, 2.5, 5 and 10 g/L)
2. pH (2, 4, 7, 8, 9 and 12)
3. Initial dye concentration (25, 100, 200, 250, 300 and 400 mg/L)
4. Time upto 150 min
5. Agitation speed (0, 50, 100, 200, 300 and 400 rpm)

2.4. Kinetic studies

Batch adsorption experiments were carried out at room temperature (25 ± 2°C). Exactly 100 mL of cationic dye solution of known initial concentration (100–400 ppm) was shaken at the agitation speed (200 rpm) with a required dose of adsorbents 2.5 g/L (SD, SD1 and SD2) for a specific period of contact time 150 min in an orbital shaker, after noting down the initial pH of the solution to the optimum pH (8). Samples were withdrawn at different time intervals.

2.5. Uptake isotherm

The dye equilibrium isotherms were determined by contacting 2.5 g/L of adsorbents (SD, SD1 and SD2) with a range of different concentrations of MB dye solutions: 10–400 mg/L. The mixture obtained was agitated at 200 rpm in a series of 250 mL conical flasks with equal volumes of solution 100 mL for a period of 90 min at room temperature 25 ± 2°C at the reaction mixture pH was 8. The contact time was previously determined by kinetic tests using the same conditions.

After equilibrium, the final concentration (C_e) was measured.

The adsorption capacity q_e (mg/g) after equilibrium was calculated by mass balance relationship equation as follows:

$$q_e = (C_o - C_e) \times (V/W) \quad (4)$$

where C_e is the equilibrium dye concentration (mg/L).

3. Results and discussion

3.1. Characteristics of adsorbing material

3.1.1. Scanning electron microscope (SEM)

A SEM was used to examine the surface of the three adsorbents using Jeol JSM-6360 LA analytical SEM and the sample was prepared by coating with gold. SEM photographs (Fig. 2) shows progressive changes in the surface of the particles. There were decrease in the thickness of the plant boundary walls in the order SD1 >> SD2 due to the treatment and also a widening in the cavities which may explain the increase in the efficiency of the treated Oak sawdust.

3.1.2. Thermogravimetric analysis

Thermogravimetric analysis TGA was carried out on different types of Oak sawdust using TGA-50 Shimatzu, Japan, analyzer under nitrogen atmosphere with 20 mL/min flow rate and 10°C/min temperature rate and was illustrated in (Fig. 3).

The TGA analysis showed weight loss at 100°C could be attributed to the loss of water from samples. Also the thermal stability of the untreated sawdust and the treated sawdust either with acid or base almost unchanged.

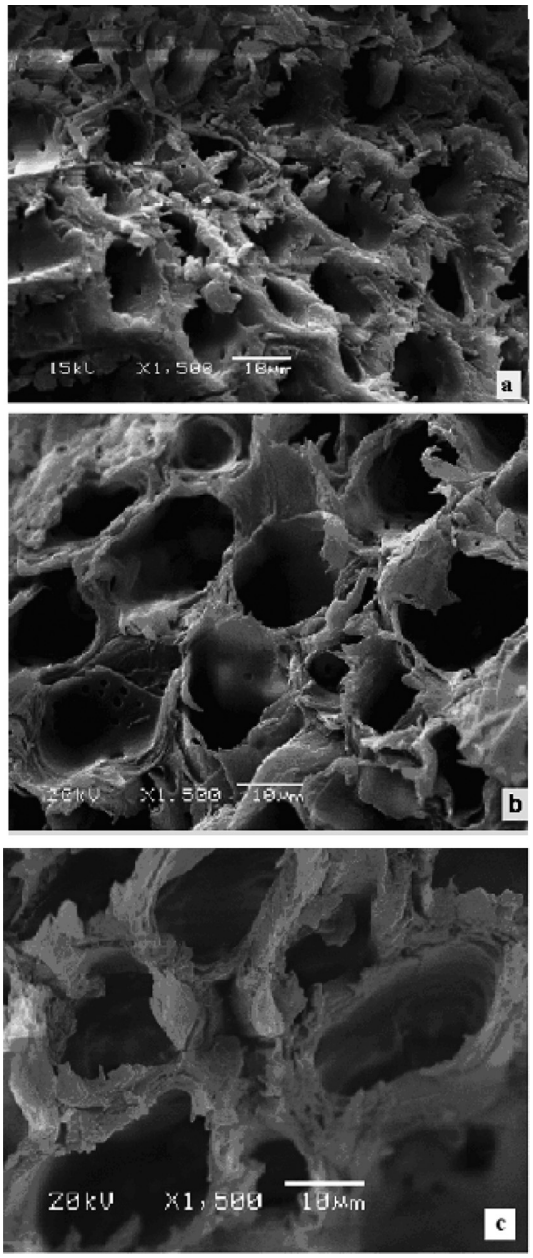

Fig. 2. Scanning electron micrographs of three Oak sawdust adsorbents: [a] SD, [b] SD1 and [c] SD2.

3.1.3. FTIR analysis

FTIR analysis was performed using Fourier transfer for infrared spectrophotometer FTIR-8400 S Shimadzu, Japan, to explain the effect of hydrolysis on the efficiency of Oak sawdust and to determine the ideal hydrolyzing agent. The increase of the cation sorption capacity of wood fiber was explained in sight of the idea of saponification process of the wood fiber using base to produce carboxylate groups instead of ester groups which can bind cations as shown in the following Eq. (5) [16]:

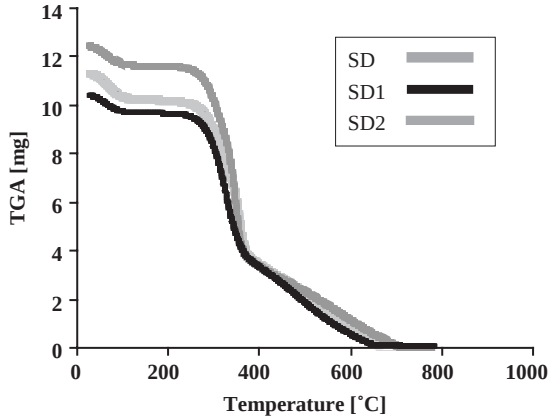

Fig. 3. TGA curves for different Oak sawdust.

$$RCOOR' + H_2O + OH^- \rightarrow RCOO^- + R'OH + H_2O \quad (5)$$

The IR bands consisted of four regions: the broad hydrogen band (3200–3600 cm^{-1}), C–H stretching region (2800–3000 cm^{-1}), carbonyl group stretching region (1550–1750 cm^{-1}), and fingerprint bands (below 1550 cm^{-1}). In finger print region absorption cannot clearly be assigned to any particular vibration because they correspond to complex interacting vibration systems. The region between 1800 and 3500 cm^{-1} presents two major peaks centered at about 3420 cm^{-1} (the H-bonded OH group) and at 2921 cm^{-1} (the C–H stretching of the CH_2 groups). The region between 1500 and 1800 cm^{-1} is a special range to evaluate the degree of saponification since this represents the carbonyl and double bond region [17–19].

All spectra were set at the base line equally and then, this range was magnified to investigate this region more closely. In this range, there are two peaks centered at 1620 and 1737 cm^{-1}. According to the literature [17–20], the peak wavenumber of the ester group and carboxyl acid groups in the organic compounds is approximately 1740 cm^{-1} while the peak wavenumber of the carboxylate ion groups is about 1620 cm^{-1}. Barker and Owen [21] assigned carboxyl groups a peak number of 1737 cm^{-1}, and Brown et al. [22] assigned a peak number of 1620 cm^{-1} as a carboxylate. These peak numbers are identical to the numbers in this study. Therefore, it can be concluded from Fig. 4 that the peak at 1737 cm^{-1} is attributed to the absorption of carboxylic acid ester groups in SD, SD1 and SD2 while the peak at 1620 cm^{-1} corresponds to the absorption of the carboxylate. In SD1 which is treated with NaOH, this peak is much more greater than the other two SDs while this increase of the carboxylate group peak accompanied with decrease in the carboxylic acid

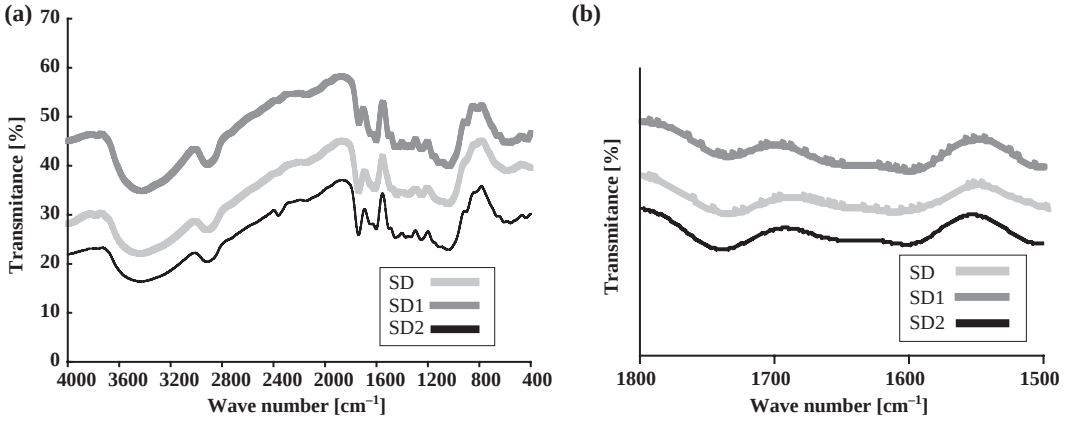

Fig. 4. [a] FTIR spectra of different treated and untreated Oak sawdust. [b] FTIR spectra of the carbonyl group region from 1500 to 1800.

group peak indicating the saponification of the carboxylic acid ester groups into carboxylate groups. Meanwhile, the sawdust treated with acid there were almost no change in the intensity of the two peaks.

3.1.4. Physical characteristics

Table 1 shows the physical characteristics of the three adsorbents used in the present study.

3.2. Investigation of adsorption parameters

3.2.1. Effect of pH

The pH of the solution has a significant impact on the uptake of MB, since it determines the surface charge of the adsorbent, the degree of ionization of the adsorbate. In order to establish the effect of pH on the biosorption MB, the batch adsorption studies at different pH values were carried out after an adsorption period of 30 min in the pH range of 2–12 (Fig. 5).

Fig. 5 shows that the maximum percent removal MB on the adsorbents was observed at pH 8 and significantly decreased by reducing the pH values and slightly decreased at higher pH values. Little sorption at lower pH could be ascribed to the hydrogen ions competing with MB for sorption sites [23–25]. This means that at higher H^+ concentration, the biosorbent surface becomes more positively charged, thus, reducing the attraction between adsorbent and MB. In contrast as the pH increases, more negatively charged surface become available, thus, facilitating greater MB uptake [26]. At a higher pH, the percentage removal of MB dye decreased and it could be attributed to decrease in the solubility of the dye [27]. Also, it was observed that at constant pH, the percent removal

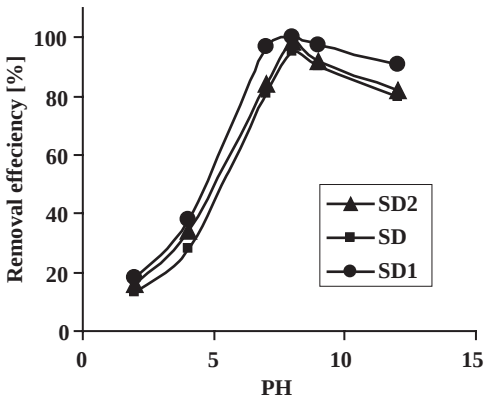

Fig. 5. Effect of the different pH on the removal of MB dye onto different adsorbents (initial dye concentration = 50 ppm, adsorbent dose = 2.5 g L^{-1}, contact time = 30 min, solution temp. = 25 ± 2°C and agitation speed = 200 rpm).

Table 1
Physical properties of the different types of adsorbents

Adsorbent type	Ash content [%wt]	Moisture content [%wt]	Bulk density [kg/m^3]	Soluble hemicellulose content [%]	Yield [%]
SD	0.17	8.54	1000	16	–
SD1	0.9	5.902	952	–	74
SD2	0.16	5.764	1000	–	80

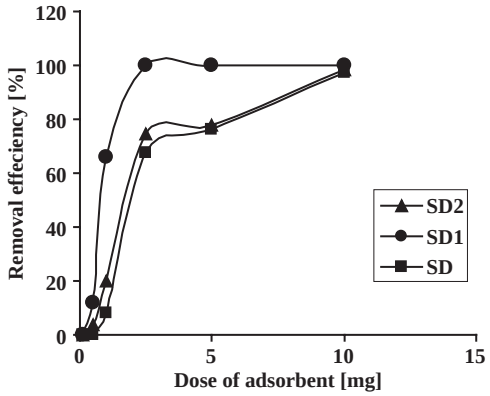

Fig. 6. Effect of adsorbent dose on the removal of MB dye onto different adsorbents (initial dye concentration = 50 ppm, contact time = 30 min, pH = 7, solution temp. = 25 ± 2°C and agitation speed = 200 rpm).

increased in the order of SD1 > SD2 > SD and this means that the chemically treated adsorbent is favorable for dye removal. This is attributed to the fact that the surface of oxidized adsorbent has a larger negatively charge than that of non-oxidized one [28].

3.2.2. Effect of adsorbent dose

One of the parameters that strongly affect the sorption removal is the dose of the adsorbents. With the fixed cationic dye concentration, it can be easily inferred that the percent removal of cationic dye increases with increasing weight of all type of adsorbents as shown from Fig. 6.

This may be due to the increase in availability of surface active sites resulting from the increased dose of the adsorbent [1,29]. Also, it was observed that at constant adsorbent dose, the percent removal increased in the order of SD1 >> SD2 > SD and this means that the chemically treated adsorbent is favorable for dye removal.

Also it was found that the removal efficiency of MB dye on the base treated sawdust is greater than the untreated and acid-treated sawdust, it could be explained by the effect of the base on sawdust ester function groups. Saponification of ester by NaOH produced carboxylic acid groups and thus increasing the negative charge on the surface of sawdust and consequently increase the efficiency of removing cationic dye.

3.2.3. Effect of contact time

The effect of contact time on the percentage removal of MB dye was investigated at initial dye concentration (25–400 mg/L) onto SD, SD1 and SD2 adsorbents as shown in Fig. 7.

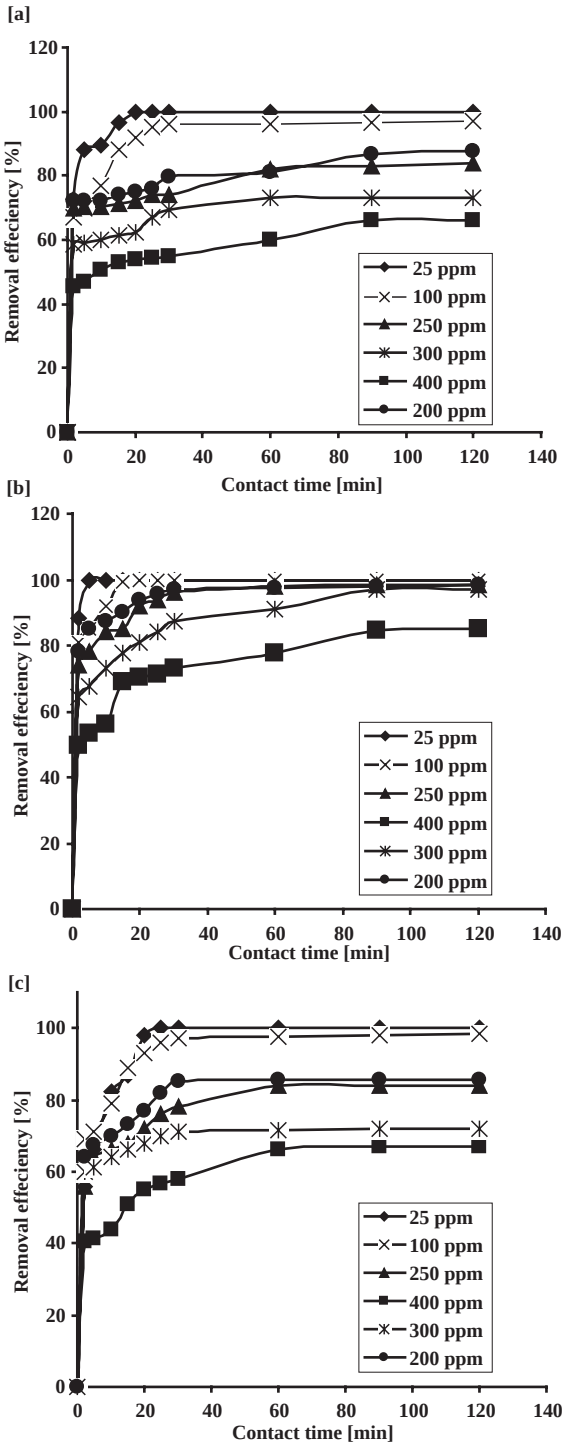

Fig. 7. Effect of contact time on the removal of MB dye onto SD using different initial dye concentrations (adsorbent dose = 2.5 g L^{-1}, pH = 8, solution temp. = 25 ± 2°C and agitation speed = 200 rpm). [a] SD, [b] SD1 and [c] SD2.

The pattern of graphs was almost same for different dye concentrations and for all type of adsorbents. The plots reveal that the removal of cationic dye MB

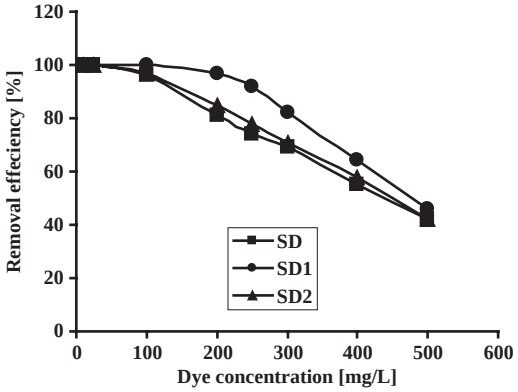

Fig. 8. Effect of initial dye concentration on the removal of MB dye onto different adsorbents (adsorbent dose = 2.5 g L^{-1}, pH = 8, solution temp. = 25 ± 2°C, contact time = 30 min and agitation speed = 200 rpm).

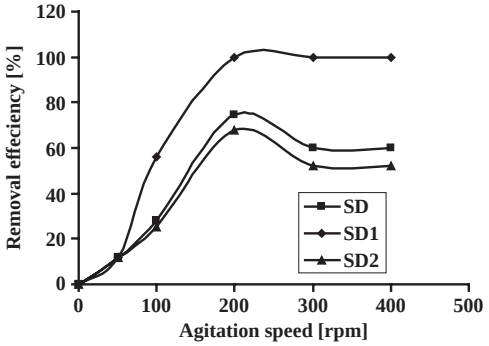

Fig. 9. Effect of the agitation speed on the removal of MB dye onto different adsorbents (initial dye concentration = 50 ppm, adsorbent dose = 2.5 g L^{-1}, pH = 7, contact time = 30 min and solution temp. = 25 ± 2°C).

increases with time and attains saturation in about 90 min. Basically, the removal of dye is rapid, but it gradually decreases with time until it reaches equilibrium (90 min). MB showed a fast rate of sorption during the first 5 min of the sorbate–sorbent contact and the rate of percent removal becomes almost insignificant due to a quick exhaustion of the adsorption sites. The rate of percent dye removal is higher in the beginning due to a larger surface area of the adsorbent being available for the adsorption of the dye. After adsorption, the rate of dye transported from the exterior to the interior sites of the adsorbent particles. The two stage sorption mechanism with the first rapid and quantitatively predominant and the second slower and quantitatively insignificant, has been extensively reported in literature [19].

3.2.4. Effect of initial dye concentration

The effect of initial dye concentration on the removal of MB dye (in terms of percentage removal) on various adsorbents was studied as shown in Fig. 8. The percentage removal of the dye was found to decrease with the increase in initial dye concentration. This indicates that there was reductions in immediate solute adsorption, owing to the lack of available active sites required for the high initial concentration of MB. Similar results have been reported in literature [24,25,30]. The results show that the percentage removal of dye decreases from 100 to 55, 100 to 73 and 100 to 58 as the initial dye concentration increases from 25 up to 400 ppm for 2.5 g/L of SD, SD1 and SD2, respectively. Also, the figure indicates that SD1 has the maximum percentage removal of all types used.

3.2.5. Effect of agitation speed

Agitation is an important parameter in sorption phenomena, influencing the distribution of the solute in the bulk solution and the formation of the external boundary film. The effect of agitation speed (in rpm) on the % removal of the original dye concentration was investigated in Fig. 9. The % removal seemed to be affected by the agitation speed for values between 0 and 200 rpm, thus confirming that the influence of external diffusion on the sorption kinetic control plays a significant role. Also it is clear that while increasing mixing rate from 200 to 300 rpm, % removal decreased from 74.6 to 60 and 67.6 to 52 for SD and SD2, respectively. This decrease may be attributed to an increase desorption tendency of dye molecules and/or having similar speed of adsorbent particles and adsorbate ions (i.e. the formation of a more stable film around the adsorbent particles). In contrast, the small effect of agitation in the range of 200–400 rpm showed that external mass transfer was not the rate-limiting step, and implied that intra-particle diffusion resistance needed to be included in the analysis of overall sorption. This also indicates that a 200 rpm shaking rate is sufficient to assure that all the surface binding sites are made readily available for dye uptake. Then the effect of external film diffusion on adsorption rate can be assumed to be not significant. The results were in agreement with Batzias and Sidiras [31].

All adsorption parameters were studied in accordance with the characterization results of the untreated and treated oak sawdust. Where SD1 gives higher efficiency than SD2 and SD Which could be attributed to the pores widening due to the treatment and the solvolysis of the constituent of the boundary walls.

Table 2
Langmuir, Freundlich and Temkin adsorption constants for different adsorbent materials

	Langmuir			*Freundlish*			*Temkin*		
Type of adsorbent	q_o	k	R^2	K_f	1/n	R^2	R^2	a	b
SD	86.96	-2.17	0.989	34.3	0.2	0.802	0.976	-0.77	0.056
SD1	92.59	-0.476	0.995	93.2	0.03	0.065	0.933	20.77	0.611
SD2	86.96	-2.17	0.989	22	0.29	0.569	0.934	-1.36	0.062

3.3. Adsorption isotherms

In order to optimize the design of an adsorption system to remove the dye, it is important to establish the most appropriate correlations for the equilibrium data for each system. In this study, the experimental isotherm data set obtained was fitted using adsorption models including Langmuir, Freundlich and Temkin isotherm.

The applicability of the isotherm equations is compared by judging the correlation coefficient, R^2.

3.3.1. Langmuir adsorption model

Langmuir isotherm is based on the theoretical principle that only a single adsorption layer exists on an adsorbent and it represents the equilibrium distribution of dye between the solid and liquid phases. The basic assumption of the Langmuir adsorption process is the formation of a monolayer and after that no further adsorption takes place.

The equation is described by

$$q_e = x/m = q_o k c_e/(k c_e + 1) \quad (6)$$

where x is the amount of dye adsorbed, m is the unit mass of adsorbent, and q_e is the amount of dye adsorbed per unit mass of adsorbent; q_o and k are Langmuir constants, and are the significance of adsorption capacity (mg/g) and energy of adsorption (L/mg) respectively; and C_e is the equilibrium concentration of adsorbate after adsorption (mg/L); q_o is the maximum adsorption capacity corresponding to complete monolayer coverage (mg of adsorbate per g of adsorbent). Eq. (6) can be re-arranged to yield:

$$c_e/q_e = c_e/q_o + 1/q_o k \quad (7)$$

The linearized Langmuir isotherms allows the calculation of adsorption capacities and the Langmuir constants. The values of q_o and k were determined from the intercept and slope of the linear plot of C_e/q_e and C_e (Table 2). Fig. 10 shows the adsorption Langmuir isotherms of MB dye on the different adsorbents used (SD, SD1, SD2). The good fit of the experimental data and the correlation coefficients R^2 higher than 0.98 indicated the applicability of the Langmuir isotherm model.

The essential characteristics of Langmuir dimensionless constant separation factor or equilibrium parameter, R_L, which is defined by the following equation [32]:

$$R_L = 1/1 + k\,C_o \quad (8)$$

where C_o is the initial dye concentration, mg/L.

In the present study, the values of R_L (Table 3) are observed to be in the range 0–1, indicating that the adsorption process is favorable for all types of adsorbents.

3.3.2. Freundlich model

Freundlich adsorption isotherm is an indicator of the extent of heterogeneity of the adsorbent surface. Freundlich adsorption model stipulates that the ratio

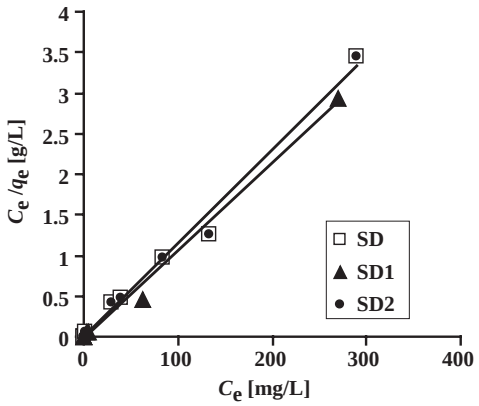

Fig. 10. Langmuir isotherm plot for adsorption of MB dye onto different adsorbents.

Table 3
R_L values for different adsorbents

	Value of R_L		
Dye concentration (ppm)	SD	SD1	SD2
10	0.044	0.174	0.044
25	0.018	0.078	0.010
100	4.59×10^{-3}	0.021	4.59×10^{-3}
200	2.3×10^{-3}	0.01	2.3×10^{-3}
250	1.84×10^{-3}	8.33×10^{-3}	1.84×10^{-3}
300	1.53×10^{-3}	6.95×10^{-3}	1.53×10^{-3}
400	1.15×10^{-3}	5.22×10^{-3}	1.15×10^{-3}

of solute adsorbed to the solute concentration is a function of the solution. The empirical model was shown to be consistent with an exponential distribution of active centers, characteristic of heterogeneous surfaces. The amount of solute adsorbed, q_e, is related to the equilibrium concentration of solute in solution, C_e, following:

$$q_e = k_f c_e^{1/n} \tag{9}$$

This expression can be linearized to give the following equation:

$$\log q_e = \log k_f + 1/n \log c_e \tag{10}$$

where k_f is a constant for the system, related to the bonding energy. k_f can be defined as the adsorption or distribution coefficient and respects the quantity of dye adsorbed onto adsorbents for a unit equilibrium concentration (a measure of adsorption capacity, mg g^{-1}). The slope $1/n$, ranging between 0 and 1, is a measure of adsorption intensity or surface heterogeneity, becoming more heterogeneous as its value gets closer to zero [33]. A value for $1/n$ below 1 indicates a normal Frendlich isotherm while $1/n$ above 1 is an indicative of cooperative adsorption [34]. A plot of log (q_e) vs. log (C_e) (figure not include), where the values of k_f and $1/n$ are determined from the intercept and slope of the linear regressions (Table 2) for all type of adsorbents. The low values of R^2 (<90%) for all type of adsorbents show that the adsorption of MB dye on the different adsorbents used could not be well described by Freundlich isotherms.

3.3.3. Temkin model

Temkin considered the effects of indirect adsorbent/adsorbate interactions on adsorption isotherms. The heat of adsorption of all the molecules in the layer would decrease linearly with coverage due to adsorbent/adsorbate interactions [35]. The Temkin isotherm has been used in the form as follows:

$$q_e = a + b \ln C_e \tag{11}$$

Therefore a plot of q_e vs. ln C_e enables one to determine the constants to a and b as shown from the slope and intercept in Fig. 11. When the a value is larger, this means that the adsorbent/adsorbate interaction is also larger [36].

The applicability of the three isotherm's models for the present data approximately follow the order: Langmuir > Temkin >> Freundlich, in case of MB dye on the different adsorbents.

3.4. Adsorption kinetics

The study of the adsorption kinetics is the main factor for designing an appropriate adsorption system and quantifying the changes in adsorption with time requires that an appropriate kinetic model is used.

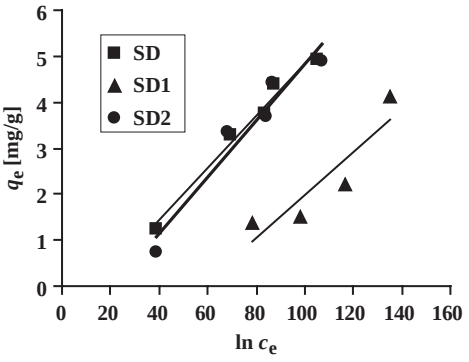

Fig. 11. Temkin Isotherm plot for adsorption of MB dye onto different adsorbents.

In order to analyze the adsorption kinetics of MB dye, the pseudo-first-order, pseudo-second-order and simple Elovich kinetic models were applied to data [37]. The first-order rate equation of Lagergren is one of the most widely used for the sorption of a solute from liquid solution [38] and is represented as:

$$\ln(q_e - q_t) = \ln q_e - k_1 t \quad (12)$$

where q_e is the mass of dye adsorbed at equilibrium (mg/g), q_t is the mass of dye adsorbed at time t (mg/g), k_1 is the first-order reaction rate constant (min^{-1}). The pseudo-first order considers the rate of occupation of adsorption sites to be proportional to the number of unoccupied sites. The first-order rate constant k_1, can be obtained from the slope of the plot $\log(q_e - q_t)$ vs. time Fig. 12. The correlation coefficients for the first-order kinetic model were not high for all adsorbents and concentrations. Also, the estimated values of q_e calculated from the equation differed from the experimental values (Table 4), which shows that the model is not appropriate to describe the adsorption process.

In addition, a pseudo-second-order equation based on adsorption equilibrium capacity may be expressed in the form [39–43]:

$$t/q_t = 1/k_2 q_e^2 + t/q_e \quad (13)$$

where k_2 is the second-order reaction rate equilibrium constant (g/mg min). A plot of t/q_t against t should give a linear relationship for the applicability of the second-order kinetic. Fig. 13 shows the linearlized form of the pseudo-second-order model for the adsorption of different initial concentrations MB dye on SD, SD1 and SD2. The correlation coefficients were more than 0.98, suggest a strong relationship between the parameters and also explains that the process follows pseudo-second-order kinetics. The correlation coefficients, R^2, the pseudo-second-order rate parameters and the estimated values of q_e calculated from the equation are shown in Table 4.

Finally, Eq. (14) will be used to test the applicability of the Elovich equation to the kinetics of basic dye adsorption. The simple Elovich model may be expressed in the form [44]:

$$q_t = A + B \ln t \quad (14)$$

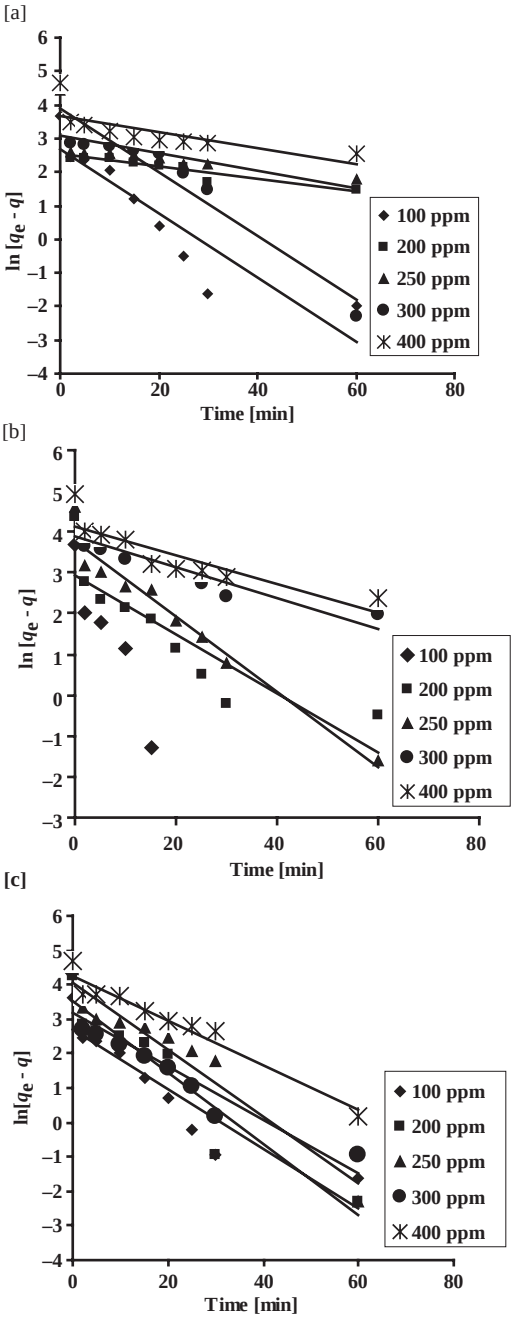

Fig. 12. First-order plots of MB dye adsorption onto different adsorbents: [a] SD, [b] SD1 and [c] SD2.

where A represents the rate of chemisorptions at zero coverage (mg/g min) and B is related to the extent of the surface coverage and activation energy for chemisorptions (g/mg).

The plot of q_t vs. ln t should give a linear relationship for the applicability of the simple Elovich kinetic. The results are also shown in Fig. 14 as a plot of q_t

Table 4
Comparison of the first- and second-order adsorption rate constants and calculated and experimental q_e values for different adsorbents.

			1st order			*2nd order*		
Type of adsorbent	***Dye concentration (ppm)***	$q_{e\ exp.}$	R^2	k_1	qe_{calc}	R^2	K_2	qe_{calc}
	100	38.6	0.834	0.0954	14.36	0.9982	0.02	39.37
	200	69.2	0.892	0.0184	12.47	0.999	0.022	64.52
SD	250	83.2	0.44	0.026	21.51	0.9951	$9.4*10^{-3}$	81.3
	300	87.6	0.353	0.026	22.83	0.9952	$6.45*10^{-3}$	88.5
	400	105.4	0.543	0.024	39.46	0.9988	$9.33*10^{-3}$	92.59
	100	40	0.90	0.28	26.39	0.9994	0.0691	40.32
	200	78.4	0.77	0.073	19.08	0.9994	0.018	78.1
SD1	250	98.2	0.95	0.092	43.05	0.9979	$7.3*10^{-3}$	100
	300	116.4	0.77	0.038	48.42	0.9979	$5.84*10^{-3}$	108.7
	400	135.2	0.77	0.036	62.78	0.9958	$3.2*10^{-3}$	128.2
	100	39.16	0.86	0.086	14.57	0.998	0.019	40
	200	68.44	0.90	0.104	33.56	0.9933	0.012	69.93
SD2	250	84	0.93	0.0973	59.1	0.9958	$5.6*10^{-3}$	84.75
	300	86.4	0.82	0.077	24.11	0.9992	0.013	86.96
	400	106.8	0.95	0.055	71.76	0.982	$3.09*10^{-3}$	108.7

against ln(t) for the adsorption of different initial concentrations of MB dye on SD, SD1 and SD2 for the Elovich equation. The Elovich equation parameter can be obtained from the slope and intercept of the plot q_t vs. ln t. The correlation coefficients, R^2, and the Elovich equation parameters, A and B, are shown in Table 5. Comparison of the three models reveals that the R^2 for first order, pseudo-second-order and the Elovich equations show that the results can be well represented by the pseudo-second-order model.

Hence, on the basis of the excellent fit of the pseudo-second order and the correlation of the experimental results with the pseudo-second-order model, the main adsorption mechanism is probably a chemisorption reaction.

3.5. Intra-particle diffusion model

The adsorption mechanism of a sorbate onto the adsorbent follows three steps viz. film diffusion, pore diffusion and intra-particle transport. The slowest of the three steps controls the overall rate of the process. Generally, pore diffusion and intra-particle diffusion are often rate-limiting in a batch reactor, which for a continuous flow system film diffusion is more likely the rate-limiting step [45]. The adsorption rate parameter which controls the batch process for most of the contact time is the intra-particle diffusion [4,46]. The possibility of intra-particle diffusion resistance affecting adsorption was explored by using the intra-particle diffusion model as:

$$q_t = k_{ad} t^{1/2} + I \tag{15}$$

where k_{ad} is the intra-particle diffusion rate constant (mg g^{-1} $min^{-1/2}$). In Fig. 15, a plot of q_t (mg/g) vs. $t^{1/2}$ ($min^{-1/2}$) are presented for all adsorbents. Values of I (Table 6) give an idea about the thickness of the boundary layer, i.e., the larger intercept the greater is the boundary layer effect [30]. The deviation of straight lines from the origin, as shown in the figure, may be because of the difference between the rate of mass transfer in the initial and final steps of adsorption. Further, such deviation of straight line from the origin indicates that the pore diffusion is not the sole rate-controlling step [4]. From Fig. 15, it may be seen that there are two separate regions, the first portion is attributed to the bulk diffusion and the second portion to intra-particle diffusion [47]. The values of k_{ad} as obtained from the slopes of the straight line are listed in Table 6. The estimated values of k_{ad} are higher for treated oak sawdust (SD1 > SD2) than for the original material (SD). The results show that the treatment enhances the adsorption rate by increasing the intra-particle diffusion rate constant. This enhancement can possibly be attributed to the removal of the hemicelluloses during sulphuric acid treatment, resulting in the 'opening' of the lignocellulosic matrix's structure.

3.6. Mechanism of adsorption

The removal of MB by adsorption on SD, SD1 and SD2 was found to be rapid at the initial period of

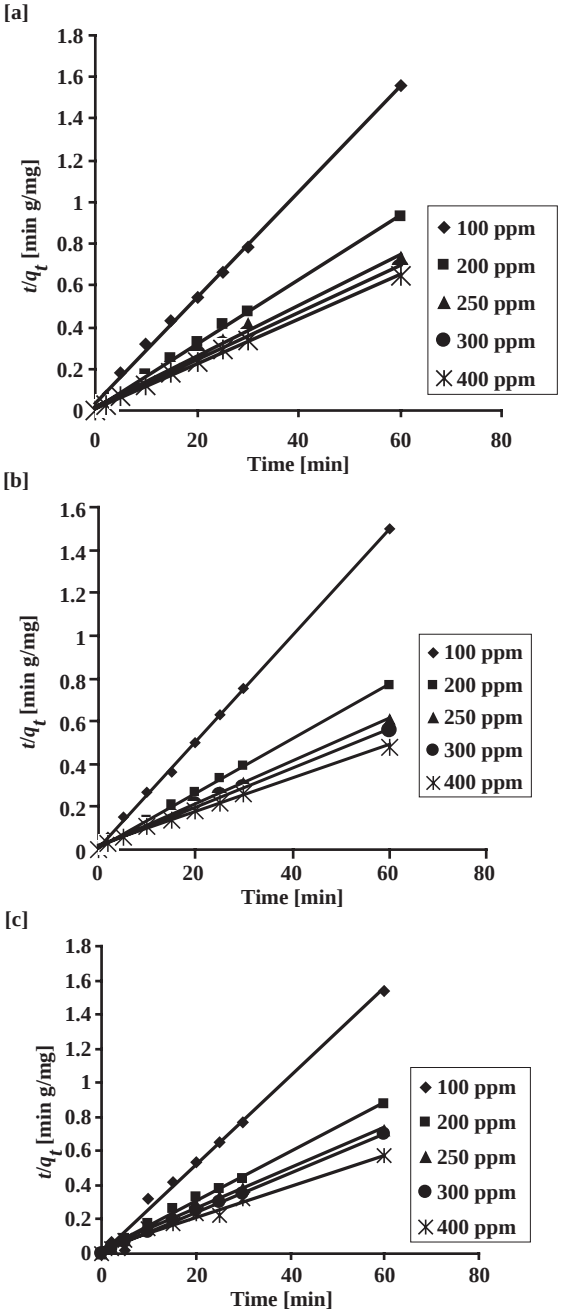

Fig. 13. Second-order plots of MB dye adsorption onto different adsorbents: [a] SD, [b] SD1 and [c] SD2.

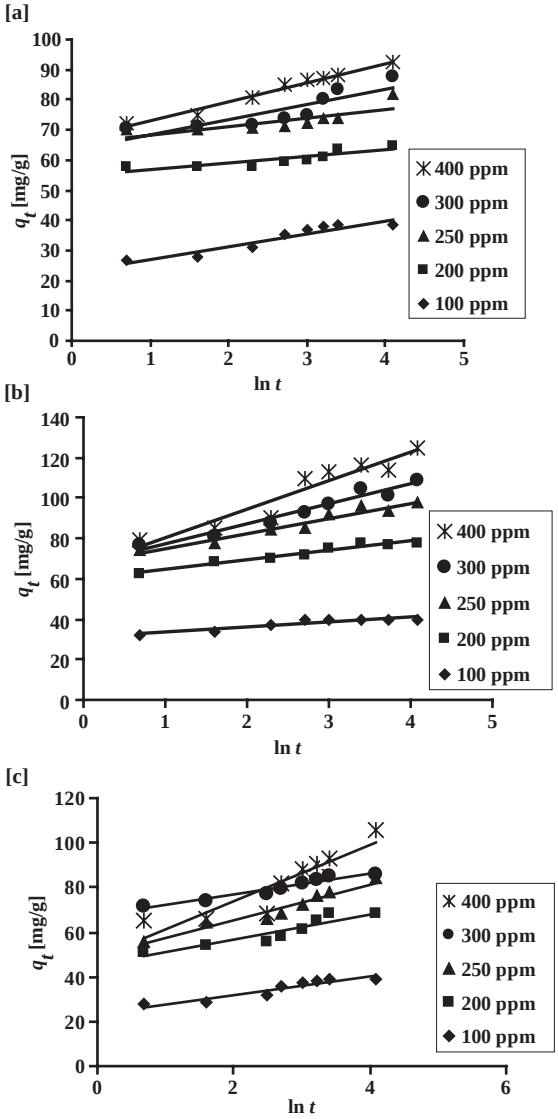

Fig. 14. Elovich plots of MB dye adsorption onto different adsorbents: [a] SD, [b] SD1 and [c] SD2.

contact time and then to become slow and stagnate with the increase in contact time. The removal of MB by adsorption on surface of SD, SD1 and SD2 was due to MB as MB^+ cationic form. The mechanism for the removal of dye by adsorption may be assumed to involve the following four steps [30]:

- Migration of dye from bulk of the solution to the surface of the adsorbent (SD, SD1 and SD2).
- Diffusion of dye through the boundary layer to the surface of the adsorbent.
- Adsorption of dye at an active site on the surface of adsorbent.
- Intra-particle diffusion of dye into the interior pores of the SD, SD1 and SD2 particle.

The boundary layer resistance will be affected by the rate of adsorption and increase in contact time, which will reduce the resistance and increase the mobility of dye during adsorption. Since, the uptake of dye at the active sites of SD, SD1 and SD2 is a rapid process in the order of SD1, SD2 and SD, the rate of adsorption is mainly governed by either liquid phase mass

Table 5
Elovich adsorption rate constants and calculated and experimental q_e values for different adsorbents

Type of adsorbent	Dye concentration (ppm)	$q_{e\ exp}$	Elovich			
			R^2	A	B	$q_{e\ calc}$
SD	100	38.6	0.899	42.08	4.27	22.88
	200	69.2	0.728	64.29	2.16	54.58
	250	83.2	0.616	75.66	2.29	65.36
	300	87.6	0.758	86.19	5.11	63.19
	400	105	0.979	95.1	6.26	66.92
SD1	100	40	0.867	42.51	2.56	30.97
	200	78.4	0.96	80.99	4.7	59.83
	250	98.2	0.948	10.27	7.54	67.35
	300	116	0.949	11.53	9.72	67.78
	400	135	0.909	129.6	14.1	66.16
SD2	100	39.2	0.884	42.22	4.14	23.6
	200	68.4	0.874	70.87	5.69	45.27
	250	84	0.94	85.27	8	49.26
	300	86.4	0.93	88.59	4.77	67.12
	400	107	0.843	105.5	12.6	48.74

transfer rate or intra-particle mass transfer rate [30]. The applicability of intra-particle diffusion model indicates, that it is the rate-determining step.

3.7. Thermodynamics

The variation in temperature, influencing the distribution of adsorbate between solid and liquid phases was examined in the range 298–333 K. Moreover the increase in dye sorption with a rise in temperature can be explained on the basis of thermodynamic parameters such as change in enthalpy (ΔH) and entropy (ΔS) which are calculated using free energy (ΔG), by using the van't Hoff [48,49]:

$$\ln\ k_c = \frac{\Delta S}{R} - \frac{\Delta H}{RT} \tag{16}$$

where $k_c = F_e/(1 - F_e)$, and $F_e = (C_o - C_e)/C_o$; is the fraction adsorbed at equilibrium, while T is the temperature in K and R is the gas constant [8.314 J (mol K^{-1})]. The plot of $\ln k_c$ vs. $1/T$ gives a straight line with acceptable coefficient of determination (R^2) as shown in Fig. 16. From the slope and the intercept of van't Hoff plots, the values of ΔH and ΔS have been computed, while the Gibbs free energy change ΔG was calculated using the following equation [50]:

$$(\Delta G) = -RT \ln k_c \tag{17}$$

The thermodynamic parameters for the sorption of MB onto (SD, SD1 and SD2) at various temperatures were calculated and summarized in Table 7. The positive values of ΔH for all type of adsorbents indicate that the studied sorption processes are endothermic in nature. Furthermore the negative values of ΔG demonstrate the spontaneous behavior of the sorption processes [50]. The decrease in the value of ΔG for each type of adsorbent with the increase of temperature shows that the reaction is more spontaneous at higher temperature which indicates that the sorption processes are favored by the increase in temperature [51]. Finally, the positive values of ΔS suggest that the increased randomness at the solid–solution interface during the sorption process. The adsorbed solvent molecules which are displaced by the adsorbate species gain more translational entropy than ions lost by adsorbate thus allowing for prevalence of randomness in the system [52]. Normally, adsorption of gases leads to a decrease in entropy due to orderly arrangement of the gas molecules on a solid surface. However, the same may not be true for the complicated system of sorption from solution [53].

Energy of activation was calculated according to a relationship between Ea and ΔH° for reactions in solution by the following equation [54]:

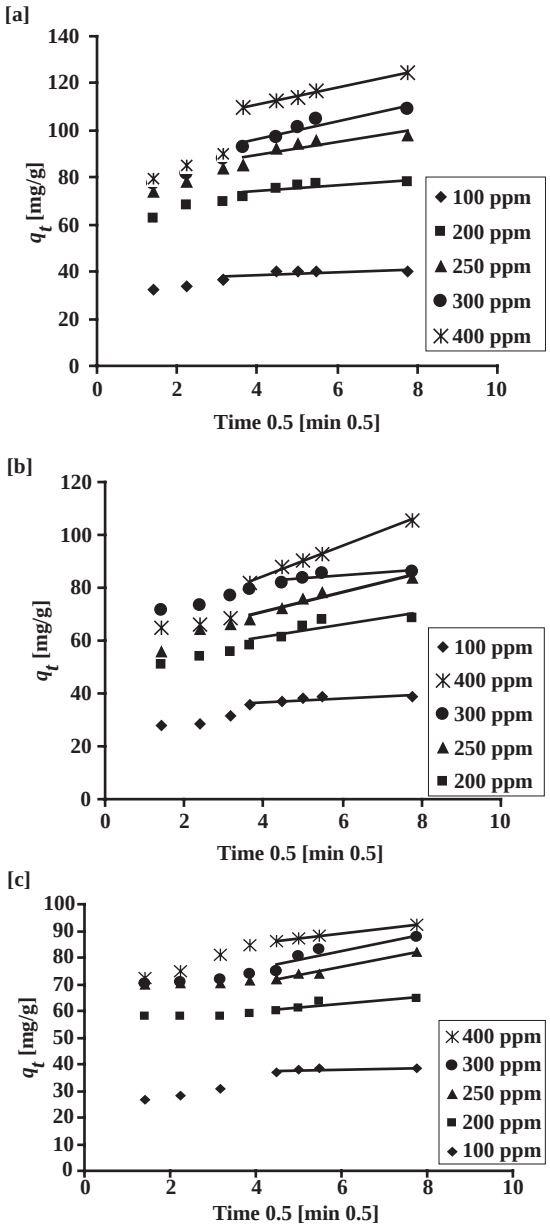

Fig. 15. Intra-particle diffusion plots of MB dye adsorption onto different adsorbents: [a] SD, [b] SD1 and [c] SD2.

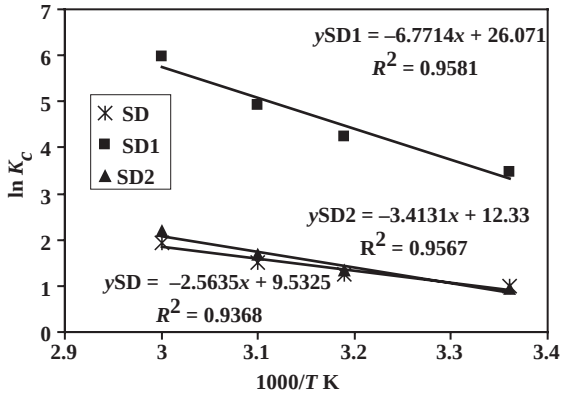

Fig. 16. Effect of temperature on MB kinetic sorption for different adsorbents (initial dye concentration = 300 ppm, adsorbent dose = 2.5 g L^{-1}, pH = 8, contact time = 90 min and agitation speed = 200 rpm).

$$Ea = \Delta H + RT \tag{18}$$

Energies of activation below 42 kJ mol^{-1} generally indicate diffusion-controlled processes and higher values represent chemical reaction processes [55–58]. In terms of *Ea*, diffusion or transport controlled reactions are those governed by mass transfer or diffusion of the adsorbate from the bulk solution to the adsorbent surface and can be described using the parabolic rate law [59]. Conversely, the reaction is surface controlled if the reaction between the adsorbate and adsorbent is slow compared with the transport or diffusion of the adsorbate to the adsorbent. For surface-controlled reactions, the concentration of the adsorbate next to the adsorbent surface is equal to the concentration of the adsorbate in the bulk solution and the kinetic relationship between time and adsorbate concentration should be linear [60]. In our study, the activation energy values were higher than 42 kJ mol^{-1} as presented in Table 7 when using SD1 as absorbent indicating chemically controlled process; also the high

Table 6
Intraparticle diffusion rate parameter at different initial dye concentration for different adsorbents

	Type of adsorbent								
	SD			SD1			SD2		
Dye concentration	k_{ad}	I	R^2	k_{ad}	I	R^2	k_{ad}	I	R^2
100	1.4107	29.34	0.5736	1.2465	32.469	0.6995	1.3604	30.071	0.6099
200	1.5846	53.215	0.8867	2.4897	62.036	0.8247	2.8103	49.118	0.7827
250	2.5798	61.134	0.954	4.1547	70.421	0.8933	4.009	54.248	0.9554
300	3.674	60.379	0.9145	4.5381	76.515	0.897	1.9384	72.593	0.804
400	2.3132	75.138	0.9342	3.5606	96.822	0.9948	5.7223	61.501	0.9942

Table 7
Thermodynamic parameters and activation energy for dye sorption onto different adsorbents

Type of adsorbent	$\triangle H$ (kJ mol^{-1})	$\triangle S$ (kJ mol^{-1})	*Ea* (kJ mol^{-1})				$\triangle G$ (kJ mol^{-1})			
			298 K	313 K	323 K	333 K	298 K	313 K	323 K	333 K
SD	21.31	79.25	23.79	23.91	24	24.08	−2.45	−3.29	−4.03	−5.39
SD1	56.3	216.75	58.78	58.9	59	59.07	−8.61	−11.07	−13.23	−16.53
SD2	28.38	102.51	30.86	30.98	31.07	31.15	−2.34	−3.44	−4.512	−6.08

values of the activation energy indicated that diffusion is not a limiting factor controlling the rate of adsorption. Consequently, adsorption of MB dye by SD1 appears to occur by chemisorption [60]. But the activation energy values were lower than 42 kJ mol^{-1} as presented in Table 7 when using SD and SD2 as absorbent indicating. The small value of the activation energy below 42 kJ mol^{-1} confirms the fact that the process of the removal MB using SD&SD2 is diffusion controlled.

4. Conclusions

In this work, Oak sawdust (SD), 0.1 N sodium hydroxide treated Oak sawdust (SD1) and 0.1 N sulphuric acid-treated Oak sawdust (SD2) were prepared and have been used successfully as an adsorbing agent for the removal of cationic MB dye from aqueous solutions. MB is found to adsorb strongly on the surface of SD1 >> SD2 > SD. The equilibrium adsorption is practically achieved in 90 min. Adsorption was influenced by various parameters such as initial pH, dose of adsorbent, contact time, initial dye concentration and agitation speed. The maximum adsorption of MB dye by SD, SD1 and SD2 occurred at an initial pH of 8.0. Removal efficiency increased with decreasing the dye concentration and increasing dose of adsorbent and agitation speed. The equilibrium sorption data are satisfactorily fitted in the order: Freundlich > Temkin > Langmuir. Adsorption kinetics follows pseudo-second-order kinetic model. Kinetic results showed that both bulk and intra-particle diffusion are effective adsorption mechanisms. Thermodynamic parameters for all type of adsorbents ΔS, ΔG and ΔH indicate that adsorption process is thermodynamically favorable, spontaneous and endothermic in nature. The process of the removal of MB using SD&SD2 is diffusion controlled while the removal of MB using SD1 is chemically controlled process. Since Oak sawdust, local furniture manufacturing company solid waste, used in this study, locally available, the adsorption process is expected to be economically viable for wastewater treatment.

Nomenclature

SD	untreated Oak sawdust
SD1	Oak sawdust treated with 0.1 M NaOH
SD2	Oak sawdust treated with 0.1 M H_2SO_4
MB	methylene blue dye
W_i	the mass of material before treated (g)
W_f	the mass of material after treated (g)
C_o	the initial dye concentration (mg/L)
C	the dye concentration at any time (mg/L)
q_e	amount of dye adsorbed at equilibrium (mg/g)
SEM	scanning electron microscope
TGA	thermogravimetric analysis
FTIR	Fourier transfer for infra red spectrophotometer
k	Langmuir constant energy of adsorption (L/mg)
q_o	Langmuir constant adsorption capacity (mg/g)
C_e	equilibrium dye concentration (mg/L)
$1/n$	sorption intensity (dimensionless)
k_f	Freundlich constant measure of adsorbent capacity (L/g)
k_1	the first-order reaction rate constant (min^{-1})
k_2	the second-order reaction rate equilibrium constant (g/mg min)
A	the rate of chemisorptions at zero coverage (mg/g min)
B	the extent of the surface coverage and activation energy for chemisorptions (g/mg)
R^2	correlation coefficient
k_{ad}	intra-particle diffusion rate constant mg g^{-1} min$^{-1/2}$
$t^{1/2}$	the square root of time (min$^{-1/2}$)
q_t	the amount of heavy metals adsorbed (mg/g)
t	time (min)
V	volume of the solution (L)

W	weight of the adsorbent (g)
R_L	Langmuir equilibrium parameter
ΔH	the enthalpy change (kJ mol^{-1})
ΔS	the entropy change (kJ mol^{-1})
ΔG	the Gibbs free energy change (kJ mol^{-1})
R	the gas constant [8.314 J (mol K^{-1})]
F_e	the fraction adsorbed at equilibrium
Ea	the activation energy (kJ mol^{-1})

References

[1] V. K. Garg, R. Gupta, A. Yadav and K. Kumar, Dye removal from aqueous solution by adsorption on treated sawdust, Bioresour. Technol., 89 (2003) 121-124.

[2] K. Kadirvelu, M. Palanival, R. Kalpana and S. Rajeswari, Activated carbon from an agricultural by-product for the treatment of dyeing industry wastewater, Bioresour. Technol., 74 (2000) 263-265.

[3] A. Shukla, Y.H. Zhang, P. Dubey and J.L. Margrave, The role of sawdust in the removal of unwanted materials from water, J. Hazard. Mater., B95 (2002) 137-152.

[4] V.J.P. Poots, G. McKay and J.J. Healy, Removal of basic dye from effluent using wood as an adsorbent, J. Water Poll. Contr. Fed., 50(5) (1978) 926-935.

[5] S.I. Abo-Elela and M.A. El-Dib, Color removal via adsorption on wood shaving, Sci. Total Environ. 66 (1987) 269-273.

[6] P. Nigam, G. Armour, I.M. Banat, D. Singh and R. Marchant, Physical removal of textile dyes from effluents and solid-state fermentation of dye-adsorbed agricultural residues. Bioresour. Technol., 72 (2000) 219-226.

[7] C. Namasivayam, M.D. Kumar and R.A. Begum, Waste coir pith – a potential biomass for the treatment of dyeing wastewaters, Biomass Bioenergy, A21 (2001) 477-483.

[8] G. Annadurai, R.-S. Juang and D.J. Lee, Use of cellulose based wastes for adsorption of dyes from aqueous solutions, J. Hazard. Mater., B92 (2002) 263-274.

[9] M.M. Nassar, Intra-particle diffusion of basic red and basic yellow dyes on palm fruit bunch, Water Sci. Technol., 40(7) (1999) 133-139.

[10] M.M. Nassar and Y.H. Magdy, Removal of different basic dyes from aqueous solutions by adsorption on palm-fruit bunch particles, Chem. Eng. J., 66 (1997) 223-226.

[11] N.A. Ibrahim, A. Hashem and M.H. Abou-Shosha, Amination of wood sawdust for removing anionic dyes from aqueous solutions, Polym.-Plast. Techol. Eng., 36(6) (1997) 963-971.

[12] C. Namasivayam, R. Radhika and S. Suba, Uptake of dyes by a promising locally available agricultural solid waste-coir pith, Waste Manage., B21 (2001) 381-387.

[13] S. Sivakumar, Rajeshwarisivaraj, P. Senthilkumar and V. Subburam, Carbon from cassava peel, an agricultural waste, as an adsorbent in the removal of dyes and metal ions from aqueous solution, Bioresour. Technol., 80 (2001) 233-235.

[14] W.T. Tsai, C.Y. Chang, M.C. Lin, S.F. Chien, H.F. Sun and M.F. Hsieh, Adsorption of acid dye onto activated carbons prepared from agricultural waste bagasse by $ZnCl_2$ activation, Chemosphere, 45 (2001) 51-58.

[15] S.J. Allen, Q. Gan, R. Matthews and P.A. Johnson, Comparison of optimized isotherm models for basic dye adsorption by kudzu, Bioresour. Technol., 88 (2003) 143-152.

[16] K.J. Tiemann, J.L. Gardea-Torresdey, G. Gamez, K. Dokken and S. Sias, Use of X-ray absorption spectroscopy and esterification to investigate Cr(III) and Ni(II) ligands in alfalfa biomass, Enviro. Sci. Technol., 33(1) (1999) 150-154.

[17] A.K. Chatjigakis, C. Pappas, N. Proxenia, O. Kalantzi, P. Rodis and M. Polissiou, FTIR spectroscopic determination of the degree of esterification of cell wall pectins from stored peaches and correlation to textural changes, Carbohydr. Polym. 37(4) (1998) 395-408.

[18] C. Pappas, P. Rodis, P.A. Tarantilis and M. Polissiou, Prediction of the pH in wood by diffuse reflectance infrared Fourier transform spectroscopy, Carbohydr. Polym., 53(7) (1998) 805-809.

[19] Y. Inbar, Y. Chen and Y. Hadar, Solid-state C-13 nuclear magnetic-resonance and infrared spectroscopy of composted organic-matter, Soil Sci. Soc. Am. J., 53(6) (1989) 1695-1701.

[20] N.P.G. Roeges, A Guide to the Complete Interpretation of Infrared Spectra of Organic Structures, Wiley and Sons, NY, 1994.

[21] B. Barker and N.L. Owen, Identifying softwoods and hardwoods by infrared spectroscopy, J. Chem. Educ., 76(12) (1999) 1706-1709.

[22] P. Brown, S. Gill and S.J. Allen, Determination of optimal peat type to potentially capture copper and cadmium from solution, Water Environ. Res., 73(3) (2001) 351-362.

[23] N. Deo and M. Ali, Adsorption by a new low cost material: congo red 1 and 2, Indian J. Environ. Protec., 17(5) (1997) 328.

[24] G. McKay, M.S. Otterburn and J.A. Aja, Fullter's earth and fired clay as adsorbents for dyes stuffs, Water Air Soil Pollut., 24 (1985) 307.

[25] K.S. Low, C.K. Lee and K.P. Lee, Sorption of copper by dye-treated oil-palm fibers, Bioresour. Technol., 44 (1993) 109-112.

[26] J. Chang, R. Law and C. Chang, Biosorption of lead, copper and cadmium by biomass of *Pseudomonas aeruginosa*, Water Res., 31 (1997) 1651-1658.

[27] M. Sarioglu and A. Atay, Removal of methyllene blue by using biosolid, Global NEST J., 8(2) (2006) 113-120.

[28] D. Aggarwal, M. Goyal and R.C. Bansal, Adsorption of chromium by activated carbon from aqueous solution, Carbon, 37 (1999) 1989-1997.

[29] A. Saeed, M.W. Akhter and M. Iqbal, Removal and recovery of heavy metals from aqueous solution using papaya wood as a new biosorbent, Separat. Purif. Technol., 45 (2005) 25-31.

[30] N. Kannan and M.M. Sundaram, Kinetics and mechanism of removal of methylene blue by adsorption on various carbons – a comparative study, Dyes Pigments, 51 (2001) 25-40.

[31] F.A. Batzias and D.K. Sidiras, Dye adsorption by prehydrolysed beech sawdust in batch and fixed-bed systems, Bioresour. Technol., 98 (2007) 1053-1062.

[32] T.W. Weber and P.K. Chakraborty, Pore and solid diffusion model for fixed bed adsorbent, J. Am. Inst. Chem. Eng., 20 (1974) 228-233.

[33] F. Haghseresht and G. Lu, Adsorption characteristics of phenolic compound onto coal-reject-derived adsorbents, Energy Fuels, 12 (1998) 1100-1107.

[34] K. Fytianos, E. Voudrias and E. Kokkalis, Sorption–desorption behavior of 2,4-dichlorophenol by marine sediments, Chemosphere, 40 (2000) 3-6.

[35] B.H. Hameeda, L.H. China and S. Rengarajb, Adsorption of 4-chlorophenol onto activated carbon prepared from rattan sawdust, Desalination, 225 (2008) 185-198.

[36] I.A.W. Tan, A.L. Ahmad and B.H. Hameed, Adsorption of basic dye using activated carbon prepared from oil palm shell: batch and fixed bed studies, Desalination, 225 (2008) 13-28.

[37] E.-S.Z. El-Ashtoukhy, N.K. Amin and O. Abdelwahab, Removal of lead(II) and copper(II) from aqueous solution using pomegranate peel as a new adsorbent, Desalination, 223 (2008) 162-173.

[38] W. Jianlong, Z. Xinmin, D. Decai and Z. Ding, Bioadsorption of lead(II) from aqueous solution by fungal biomass of *Aspergillus niger*, J. Biotechnol., 87 (2001) 273.

[39] R.L. Tseng, F.C. Wu and R.S. Juang, Liquid-phase adsorption of dyes and phenols using pinewood-based activated carbons, Carbon, 41 (2003) 487-495.

[40] Y.S. Ho, G. McKay, Sorption of dye from aqueous solution by peat, Chem. Eng. J., 70 (1998) 115-124.

[41] Y.S. Ho and G. McKay, Sorption of dyes and copper ions onto biosorbents, Process Biochem., 38 (2003) 1047-1061.

[42] Y.S. Ho and C.C. Chiang, Sorption studies of acid dye by mixed sorbents, Adsorption, 7 (2001) 139-147.

[43] Y.S. Ho and G. McKay, The kinetics of sorption of divalent metal ions onto sphagnum moss peat, Water Res., 24 (2000) 735-741.

[44] C.W. Cheung, J.E. porter and G. McKay, Sorption kinetics for the removal of copper and zinc from effluents using bone char, Separat. Purif. Technol., 53 (2000) 55-64.
[45] S. Coswami and U.C. Ghosh, Studies on adsorption behavior of Cr(VI) onto synthetic hydrous stannic oxide, Water SA, 31 (2005) 597-602.
[46] M.H. Kalavathy, T. Karthikeyan, S. Rajgopal and L.R. Miranda, Kinetic and isotherm studies of Cu(II) adsorption onto H_3PO_4-activated rubber wood sawdust, Colloid. Interf. Sci., 292 (2005) 354-362.
[47] S.J. Allen, G. Mckay and K.Y.H. Khader, Intraparticle diffusion of a basic dye during adsorption onto sphagnum peat, Environ. Pollut., 56 (1989) 39-50.
[48] A.E. Martell and R.M. Smith, Critical Stability Constants: Inorganic Chemistry IV, Plenum, New York, 1977.
[49] J.M. Murray and J.G. Dillard, The oxidation of cobalt(II) adsorbed on manganese dioxide, Geochim. Cosmochim. Acta, 43 (1979) 781-787.
[50] M.G. Zuhra, M.I. Bhanger, A. Mubeena, N.T. Farah and R.M. Jamil, Adsorption of methyl parathion pesticide from water using watermelon peels as a low cost adsorbent, Chem. Eng. J., 138 (2008) 616-621.
[51] M. Syed, I. Muhammad, G. Rana and K. Sadullah, Effect of Ni^{2+} loading on the mechanism of phosphate anion sorption by iron hydroxide, Separat. Purif. Technol., 59 (2008) 108-114.
[52] N. Dizge, C. Aydiner, E. Demirbas, M. Kobya and S. Kara, Adsorption of reactive dyes from aqueous solutions by fly ash: kinetic and equilibrium studies, J. Hazard. Mater., 150 (2008) 737-746.
[53] H. Oualid, S. Fethi, C. Mahdi and N. Emmanuel, Sorption of malachite green by a novel sorbent, dead leaves of plane tree: equilibrium and kinetic modeling, Chem. Eng. J., 143(1) (2008) 73-84.
[54] J.H. Noggle, Physical Chemistry, 3rd ed., vol. 11, Harper Collins Publishers, New York, 1996, p. 1108.
[55] D.L. Sparks, Kinetics of ionic reactions in clay minerals and soils, Adv. Agron., 38 (1985) 231-266.
[56] D.L. Sparks, Kinetics of Soil Chemical Processes, Academic Press, San Diego, CA, 1989, pp. 35-57.
[57] D.L. Sparks, Environmental Soil Chemistry, Academic Press, San Diego, CA, 1995, pp. 267-280.
[58] D.L. Sparks, Kinetics of reactions in pure and mixed system, in: D.L. Sparks, ed., Soil Physical Chemistry, 2nd ed., CRC Press, Boca Raton, FL, 1999, pp. 83-178.
[59] W. Stumm and R. Wollast, Coordination chemistry of weathering. Kinetics of the surface-controlled dissolution of oxide minerals, Rev. Geophys., 28 (1990) 53-90.
[60] K.G. Scheckel and D.L. Sparks, Temperature effects on nickel sorption kinetics at the mineral–water interface, Soil Sci. Soc. Am. J., 65 (2001) 685-694.